Published online 8 March 2021

Nucleic Acids Research, 2021, Vol. 49, No. 6 ***3427–3440***
doi: 10.1093/nar/gkab137

Xenogeneic silencing relies on temperature-dependent phosphorylation of the host H-NS protein in *Shewanella*

Xiaoxiao Liu[1,2], Shituan Lin[1,2,3], Tianlang Liu[1,2,3], Yiqing Zhou[1,2,3], Weiquan Wang[1,2,3], Jianyun Yao[1,2], Yunxue Guo[1,2,3], Kaihao Tang[1,2], Ran Chen[1,2], Michael J. Benedik[4] and Xiaoxue Wang[1,2,3,*]

[1]Key Laboratory of Tropical Marine Bio-resources and Ecology, Guangdong Key Laboratory of Marine Materia Medica, Innovation Academy of South China Sea Ecology and Environmental Engineering, South China Sea Institute of Oceanology, Chinese Academy of Sciences, No. 1119, Haibin Road, Nansha District, Guangzhou 511458, China, [2]Southern Marine Science and Engineering Guangdong Laboratory (Guangzhou), No.1119, Haibin Road, Nansha District, Guangzhou 511458, China, [3]University of Chinese Academy of Sciences, Beijing 100049, China and [4]Department of Biology, Texas A&M University, College Station, TX 77843, USA

Received January 21, 2021; Revised February 17, 2021; Editorial Decision February 18, 2021; Accepted February 20, 2021

ABSTRACT

Lateral gene transfer (LGT) plays a key role in shaping the genome evolution and environmental adaptation of bacteria. Xenogeneic silencing is crucial to ensure the safe acquisition of LGT genes into host pre-existing regulatory networks. We previously found that the host nucleoid structuring protein (H-NS) silences prophage CP4So at warm temperatures yet enables this prophage to excise at cold temperatures in *Shewanella oneidensis*. However, whether H-NS silences other genes and how bacteria modulate H-NS to regulate the expression of genes have not been fully elucidated. In this study, we discovered that the H-NS silences many LGT genes and the xenogeneic silencing of H-NS relies on a temperature-dependent phosphorylation at warm temperatures in *S. oneidensis*. Specifically, phosphorylation of H-NS at Ser42 is critical for silencing the cold-inducible genes including the excisionase of CP4So prophage, a cold shock protein, and a stress-related chemosensory system. By contrast, nonphosphorylated H-NS derepresses the promoter activity of these genes/operons to enable their expression at cold temperatures. Taken together, our results reveal that the posttranslational modification of H-NS can function as a regulatory switch to control LGT gene expression in host genomes to enable the host bacterium to react and thrive when environmental temperature changes.

INTRODUCTION

Lateral gene transfer (LGT) plays a prominent role in bacterial genome evolution and environmental adaptation. The acquisition of foreign genes, including phages and plasmids, is highly likely to decrease the fitness of the recipient bacterial host under normal growing conditions. It is crucial for a bacterial host to coordinate the expansion of their functional repertoire through LGT while maintaining their physiological and regulatory integrity. Xenogeneic silencing proteins in bacteria are mostly responsible for protecting cells from the detrimental effects of LGT by selectively silencing newly acquired DNA molecules (1,2). H-NS, a nucleoid-associated DNA-binding protein, is an important xenogeneic silencing factor and serves as the 'genome sentinel' in Gram-negative bacteria (3). H-NS selectively silences LGT genes, such as virulence genes or pathogenicity islands, in *Salmonella*, thereby preventing foreign genes from having deleterious effects on their host by keeping them silent until conditions permit their expression (4–6). H-NS family proteins selectively silence the prophage rac in *Escherichia coli*, Pf4 in *Pseudomonas aeruginosa* (7–10) and CP4So prophage in *Shewanella oneidensis* MR-1 (11). However, the mechanism by which bacteria modulate H-NS to control the expression of laterally transferred genes has not been fully elucidated.

Temperature fluctuation is a primary environmental stress affecting bacteria (12–15). The H-NS protein is one of the best-studied thermoregulators and is known to regulate a serial of genes at different temperatures (16–20). It was reported that >200 thermoregulated genes in *Salmonella* exhibited H-NS-dependent upregulation as the temperature increased from 25 to 37°C (21). In *E. coli*, 69% of the

*To whom correspondence should be addressed. Tel: +86 20 8926 7515; Email: xxwang@scsio.ac.cn

thermoregulated genes were determined to be controlled by H-NS (22). Bacteria living in fluctuating environments must have the capacity to sense changes in temperature and to modulate the expression of specific genes to cope with these changes (13,23,24). The current consensus among researchers is that changes in temperature affect the capacity of H-NS to form multimers that condense DNA and repress gene expression (25–28). However, little is known regarding the relationship between H-NS xenogeneic silencing and the thermoregulatory role of H-NS.

Shewanella is an important dissimilatory metal-reducing bacterial taxon that contributes to biogeochemical metal cycling and subsurface bioremediation (29). Many *Shewanella* strains are capable of extracellular electron transfer to insoluble metal oxides, which are utilized as external electron acceptors for anaerobic respiration (30). The *Shewanella* genus has been isolated from permanently near-freezing areas, such as the Arctic and the deep sea, permanently hot areas, such as hot-spring and deep-sea hydrothermal vents, and seasonally fluctuating regions, such as surface water and sediments (31). Pangenome analyses demonstrated that LGT plays a key role in shaping the genome of *Shewanella* strains and accelerating the evolution of strains. Genes of the electron transport system were distributed across a variety of *Shewanella* strains isolated from various environments (11,32–36).

Shewanella oneidensis MR-1 is a psychrotrophic model strain that was isolated from the sediment of a surface lake, Oneida Lake. In a previous study, we demonstrated that prophage CP4So excision functions as a regulatory switch to enable the survival of *S. oneidensis* at cold temperatures by controlling the activity of SsrA (small stable RNA A) and biofilm formation (11). Genome excision of CP4So in *S. oneidensis* does not lead to host lysis due to the absence of its helper P2 prophages (34,37). The genome excision of CP4So prophage directly results in a functional loss of SsrA, and the inactivation of SsrA decreases the resistance of bacterial host to various stressors (34). As we showed earlier, the CP4So-encoded toxin/antitoxin system ParE/CopA stabilizes the phage circle after excision at cold temperatures, which enables it to reintegrate at warm temperatures (38). It is critical to note the CP4So phage genome is not lost upon excision but remains as a non-integrated episome in those cells. Importantly, we also observed that H-NS silences prophage CP4So excision at warm temperatures, but this repression is alleviated at cold temperatures (11). Similarly, in the deep-sea bacterium *S. piezotolerans* WP3, H-NS silences the cold-inducible lateral flagellar system (39). These studies further demonstrate the importance of H-NS in controlling LGT in bacterial adaptation, but the environmental cues and signaling cascades that lead to prophage excision at cold temperatures have not been fully elucidated.

In this study, we describe a key process of xenogeneic silencing via a temperature-dependent posttranslational modification of the host H-NS in *S. oneidensis*. Specifically, the control of H-NS on prophage excision and other LGT-related genes/operons is modulated via H-NS phosphorylation during temperature shifts. H-NS is phosphorylated, and phosphorylated H-NS silences foreign genes at warm temperatures, while at cold temperature, H-NS remains nonphosphorylated, and nonphosphorylated H-NS derepresses foreign genes. This study illustrates a new way of decision-making for xenogeneic silencing in response to temperature shifts in bacteria.

MATERIALS AND METHODS

Bacterial strains and growth conditions

The bacterial strains and the plasmids used in this study are listed in Supplementary Table S1. Luria-Bertani (LB) was used for growing *Shewanella* and *E. coli* strains. DAP (2,6-diamino-pimelic acid) was added at a final concentration of 0.3 mM to cultivate the auxotrophic *E. coli* WM3064. Kanamycin (50 μg ml^{-1}) was used to maintain the pHGE, pBBR1MCS-2, pHGEI01 or pET28b-based plasmids. Ampicillin (50 μg ml^{-1}) and gentamycin (15 μg ml^{-1}) were used to maintain the pHGM01-based plasmids. Spectinomycin (100 μg ml^{-1}) was used to maintain the pBBR-Cre plasmid. When necessary, isopropyl-β-D-thiogalactopyranoside (IPTG) was added as an inducer.

Construction of FLAG-tagged H-NS strain

Primers used for strain construction are listed in Supplementary Table S2. Strain MR-1 H-NS^{FLAG} with the chromosomal-encoded H-NS fused with 2× Flag-tag sequence at its C-terminus was constructed using the method as previously described (34). The fused fragment was cloned into the pHGM01 to create pHGM01-H-NS::FLAG, and a chloramphenicol resistance cassette was inserted downstream of the Flag-tag to generate pHGM01-H-NS::FLAG-Cm. The construct was then introduced onto the chromosome of *S. oneidensis* by conjugation using *E. coli* WM3064/pHGM01-H-NS::FLAG-Cm as the donor strain. The chloramphenicol resistance cassette was removed by FLP-mediated recombination (40). The correct construct was confirmed by DNA sequencing of the target region.

Quantification of prophage excision

The frequency of prophage excision in the bacterial population was determined by quantitative PCR (qPCR) as previously described (11,41). The number of chromosomes that are devoid of prophage CP4So was quantified using primers (CP4So-attB-F/R) that specifically amplify the reconstituted bacterial attachment site. The number of total cells was quantified using primers (GyrB-qPCR-F/R) that specifically amplify a single-copy chromosome gene *gyrB*. Finally, frequency of prophage excision was obtained as ratio of *attB*/*gyrB* using the calculation method that was described previously (7,42).

Mutagenesis and complementation

Site-directed mutagenesis of *hns* was performed by a two-step overlap PCR method using primers listed in Supplementary Table S2. Primers used were designed with the relevant mutation site. First, the wild-type *hns* expression plasmid, pBBR1MCS-2-*hns*, containing the open reading frame region of *hns* as well as its native promoter region.

A second round of PCR was performed with primer pairs pBBR1-H-NS-FT/RT using primary PCR products as a template, and the products were ligated into pBBR1MCS-2 using the ClonExpress II One Step Cloning Kit (Vazyme, Nanjing, China). All mutants were verified by sequencing of the mutated regions. Plasmid pBBR1MCS-2-based *hns* wild-type and its mutants were introduced into *S. oneidensis* via conjugation with *E. coli* WM3064 serving as the donor strain. In-frame deletion of genes in MR-1 was constructed by homologous recombination as previously described (43). Briefly, the DNA regions flanking the upstream and downstream regions of the target gene were amplified and joined by fusion PCR. The fused fragments were cloned into the suicide plasmid pHGM01 using BP Clonase (Thermo Fisher Scientific, MA, USA). The generated suicide plasmids were introduced into *S. oneidensis* via conjugation. The correct integration of the PCR fragment into the chromosome of *S. oneidensis* was verified by PCR and DNA sequencing.

Protein purification

H-NS wild type and variants with a 6× His tag at their C-terminus were expressed and purified using pHGE-based plasmids in *S. oneidensis* Δ*hns* strain. Cells were induced for 6 h (at $A_{600} \sim 0.6$) with 0.5 mM IPTG and were then harvested and lysed at 30 kpsi by a cell disruptor (Constant Systems Ltd., Northants, UK) in lysis buffer (50 mM NaH_2PO_4, 300 mM NaCl, pH 8.0) with the addition of protease inhibitor cocktail (Sigma-Aldrich, St. Louis, MO, USA). Nickel-nitrilotriacetic acid (Ni-NTA) agarose (Qiagen, Valencia, CA, USA) was used to purify the His-tagged proteins following the manufacturer's instructions. The purified proteins were dialyzed into a buffer (20 mM Tris–HCl, 300 mM NaCl, pH 8.0) for further analysis and were quantified with a bicinchoninic acid (BCA) assay kit (Bio Teke, Beijing, China).

LC–MS/MS Analysis

The purified H-NS proteins (20 μg) was separated by 12% SDS-PAGE and visualized by Coomassie brilliant blue staining. LC–MS/MS analysis was carried out by Jingjie PTM BioLab (Hangzhou, China) Co. Ltd. Briefly, the digested peptides were extracted, dried, and subjected to Nano electrospray ionization source followed by tandem mass spectrometry (MS/MS) in Q Exactive Plus (Thermo Fisher Scientific, MA, USA) coupled online to the UPLC. The electrospray voltage applied was 2.0 kV. The m/z scan range was 350–1800 for full scan, and intact peptides were detected in the Orbitrap at a resolution of 70 000 as previously described (44). The resulting MS/MS data were processed using Proteome Discoverer 1.3 Tandem and searched against the reference proteome of MR-1. Trypsin/P was specified as cleavage enzyme allowing up to four missing cleavages. Mass error was set to 10 ppm for precursor ions and 0.02 Da for-fragment ions. Carbamidomethyl on Cys was specified as the fixed modification and oxidation on Met, phosphorylation on Ser, Thr, Tyr and acetylation on Lys were specified as variable modifications. Peptide confidence was set at high, and peptide ion score was set >20.

Western blot analysis using Phos-tag

The Phos-tag reagent can associate with the divalent cation of Mn^{2+} and form a complex with the phosphorylated proteins, thus retarding the phosphorylated protein migration (45). Hence, Phos-tag-based western blot can be used to quantify the ratio of phosphorylated versus non-phosphorylated protein in the sample. Cells were disrupted by Fast-Prep 24 instrument in lysis buffer (20 mM Tris–HCl, 300 mM NaCl, pH 8.0). The protein concentration of the cell lysates was measured using a Bradford assay with BSA as a standard (Bio Teke, Beijing, China). A total of 20 μg protein per lane was run on 12% SDS-PAGE supplemented with 50 μM phosphate-binding tag (Phos-tag) and 50 μM $MnCl_2$. After electrophoresis, the gel was transferred to a 0.2-μm PVDF membrane. The membranes were immunoblotted with anti-Flag antibody (Abmart, Shanghai, China). A horseradish peroxidase-conjugated antibody against rabbit was used as secondary antibody. Immunoreactive bands were revealed with enhanced chemiluminescence (ECL) system (Thermo Fisher Scientific, MA, USA).

Electrophoretic mobility shift assay (EMSA)

The DNA region covering the promoter region of *alpA* (237 bp), SO_1648 (229 bp) or SO_2119 (324 bp) were PCR amplified as previously described (11). After purification, the promoter DNA fragment was labeled using the Biotin 3′ End DNA Labeling Kit (Thermo Fisher Scientific, Rockford, USA) as previously described (7). A total of 0.5 pmol probe per lane were incubated with different concentrations of purified protein for 30 min at 25°C either with or without the unlabeled probe. DNA-protein complexes were electrophoresed on 6% (w/v) polyacrylamide gels in 0.5× Tris–borate–EDTA buffer. The biotin-labeled DNA probe was visualized using the Chemiluminescence Nucleic Acid Detection Module Kit (Thermo Fisher Scientific, Rockford, USA).

Analytical ultracentrifugation

Sedimentation velocity experiments were performed at 20°C in a Beckman Optima XLA ultracentrifuge equipped with absorbance optics and an An60 Ti rotor (Beckman Coulter, Fullerton, CA, USA). Radial scans of absorbance were taken at 280 nm for H-NS proteins (WT and variants), and sedimentation velocity experiments were performed at 30 000 rpm. The sedimentation coefficient was obtained using the $c(s)$ method with the Sedfit program (46).

Transcriptome sequencing and quantitative reverse transcriptase PCR (qRT-PCR)

Overnight cultures of *S. oneidensis* were diluted (A_{600} of 0.05) and then incubated at 30°C with shaking until A_{600} reached about 1.0. Subsequently, 1 ml aliquots were removed as control and the remaining cultures were shaken at 15°C for 4 h before collecting for RNA extraction. Total RNA for transcriptome sequencing or qRT-PCR was extracted using the RNAprep Pure Cell/Bacteria Kit (Tiangen, Beijing, China). Transcriptome sequencing was performed by Genedenovo Biotechnology Co., Ltd.

(Guangzhou, China) using the Illumina Novaseq 6000 platform. Raw data of two sets (Set1 and Set 2) were submitted to the NCBI SRA database under number of PRJNA599554 (Set 1) or PRJNA6695365 (Set 2). For qRT-PCR validation, RNA was digested by gDNA wiper to eliminate the DNA contamination and 50 ng RNA was used to generate cDNA using the HiScript II QRT SuperMix (Vazyme Biotech, Nanjing, China). The housekeeping gene *rrsE* (16S rRNA gene) was used as an internal control to normalize the gene expression data. Primers for qRT-PCR are listed in Supplementary Table S2.

Reporter strain construction

The *alpA* promoter region was PCR amplified and inserted in front of the full-length *lacZ* gene in plasmid pHGEI01 (40). The created plasmid pHGEI01-P*alpA* was verified by PCR and transferred into Δ*hns* host via conjugation for integration into the host chromosome. Subsequently, the integrated plasmid was eliminated by introducing a helper plasmid, pBBR-Cre. The removal of pBBR-Cre plasmid was obtained by growing these cells without antibiotics for two passages. The reporter strain Δ*hns nrfD*::PalpA-*lacZ* was verified by PCR and sequencing the target region. H-NS and its mutants were expressed using the pBBR1MCS-2 based plasmid in the reporter strain. Cells in the log phase ($A_{600} \sim 1.0$) were harvested by centrifugation and lysed by Fast-Prep 24 instrument (MP Biomedicals, CA, USA) in buffer (0.25M Tri–HCl, pH 7.5, 0.5% Triton X-100). The resulting supernatant was collected after centrifugation and used for enzyme activity assay by adding the substrate of o-nitrophenyl-β-D-galactopyranoside (ONPG) (4 mg ml^{-1}). β-galactosidase activity was measured at A_{420} nm using a Sunrise microplate reader (Tecan, Männedorf, Switzerland) and presented as Miller units.

RESULTS

Phosphorylation of H-NS in *S. oneidensis* is temperature-dependent

Previously, we observed that repression of H-NS on excision of prophage CP4So in *S. oneidensis* was relieved after temperature downshift and was recovered after temperature upshift (11). To further investigate the regulation of H-NS during temperature shifts of *S. oneidensis*, the translation of H-NS *in vivo* was probed at 30 and 15°C. To assess endogenous expression of H-NS, a FLAG tag was fused in frame at the C-terminus of H-NS in the chromosome of *S. oneidensis* to construct the MR-1 H-NS^{FLAG} strain (Supplementary Table S1). Cells were cultured at 30°C until reaching exponential phase ($A_{600} \sim 0.8$), split into two groups, and further incubated at either 30 or 15°C. Consistent with our previous result, excision of CP4So in the MR-1 H-NS^{FLAG} strain increased ~1200-fold at 24 h at the lower temperature. In contrast, CP4So stably resided in the host chromosome at 30°C (Figure 1A). This result also suggested that FLAG tagging did not affect the action of H-NS upon CP4So excision. Next, an anti-FLAG antibody was utilized to determine the endogenous expression of H-NS, and the results showed that the amounts of H-NS protein were comparable at 30 and 15°C (Supplementary Figure S1A). After that step, we investigated whether H-NS is posttranslationally modified. His-tagged H-NS was successfully purified from the Δ*hns* strain and immunoblotted with an anti-His antibody and an anti-phospho-(Ser/Thr) antibody at both temperatures. These results demonstrate that a Ser/Thr residue of H-NS was phosphorylated in *S. oneidensis* (Supplementary Figure S1B, C).

To determine the phosphorylation state of H-NS at different temperatures, Phos-tag was used, which can specifically trap the phosphorylated protein as a lower-mobility band running above the same nonphosphorylated protein band when visualized through western blot. Single colonies of MR-1 H-NS^{FLAG} cells grown overnight on fresh LB plates were inoculated into 25 ml liquid LB and further incubated with shaking at 30 or 15°C (Figure 1B). After overnight incubation ($A_{600} \sim 4.0$), a culture sample (sample 1 or sample 2, respectively) was collected for western blot analysis. To produce a temperature downshift mimicking seasonal changes, an aliquot of cells grown at 30°C was transferred into fresh LB and grown for 24 h at 15°C (sample 3). Similarly, to mimic a temperature upshift, an aliquot of cells grown at 15°C were transferred into fresh LB and grown for 24 h at 30°C (sample 4). Western blot using Phos-tag and anti-FLAG antibodies was performed, and the ratio of phosphorylated *versus* total H-NS was quantified by ImageJ software. There was a significant difference in the degree of phosphorylation of H-NS between sample 1 and sample 2. H-NS was predominantly phosphorylated at 30°C and predominantly nonphosphorylated at 15°C (Figure 1B). When the temperature shifted from 15 to 30°C, most H-NS molecules were phosphorylated after 24 h (sample 3), whereas when the temperature shifted from 30 to 15°C, only about half of the H-NS molecules were in the phosphorylated state after 24 h (sample 4). The total H-NS protein levels detected by western blot using anti-FLAG remained constant during the temperature shifts (Figure 1B). A time-course experiment is shown in Figure 1C. The degree of phosphorylation of H-NS remained high between 8 and 24 h when cultured at 30°C (samples 1–3). When downshifted from 30 to 15°C, the ratio of phosphorylated H-NS decreased from 8 to 24 h (samples 5 and 6). Taken together, these results demonstrated that H-NS was mostly phosphorylated at warm temperatures, while a significant fraction of the H-NS was nonphosphorylated at cold temperatures.

Identification of phosphorylation sites of H-NS

To identify the phosphorylation sites, His-tagged H-NS protein produced via pHGE-*hns* in *S. oneidensis* at 30°C was subjected to LC–MS/MS analysis after trypsin digestion. A total of three phosphorylation sites were found: Ser (S) residues S2, S42 and S71 (Figure 2; Supplementary Figure S2A). Specifically, fragmentation of charged ions with mass-to-charge (m/z) of 691.32898 ($z = 2^+$), 548.56873 ($z = 3^+$) and 1005.48529 ($z = 2^+$) yielded sequential b and y ion sequences that matched the sequences of three peptides, ^{2}S(p)EFLEILTHGR^{12}, ^{41}ES(p)MEAEELQAIAAR^{54} and ^{63}QQMEAVGLS(p)IDDLGGVAVK^{81}, of H-NS with phosphate modification (representing an addition of 80 Da) (Supplementary Figure S2A). The secondary structure of

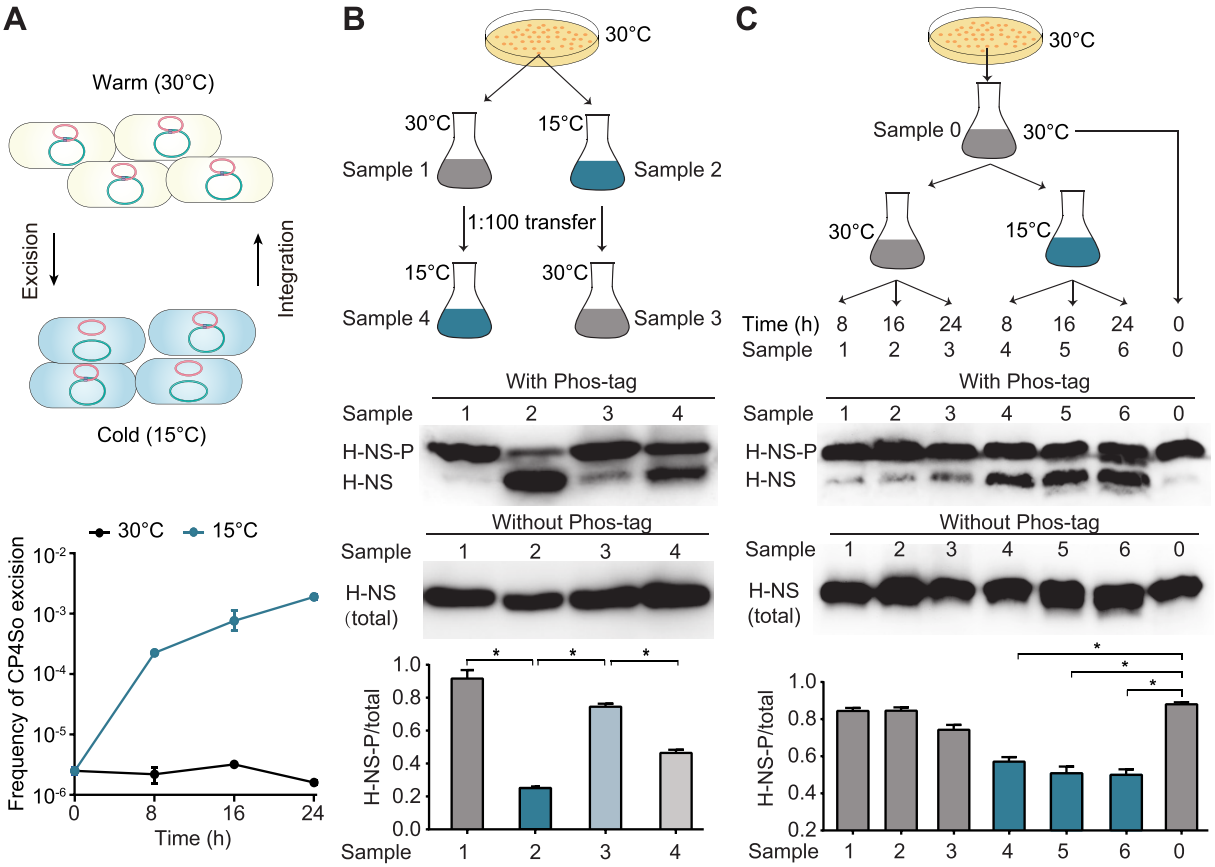

Figure 1. H-NS is phosphorylated in a temperature-dependent manner. (**A**) Excision frequency of CP4So in strain MR-1 H-NS^{FLAG} cultured at 30 or 15°C at different time points was quantified by qPCR. Experiments were performed with three independent cultures and error bars indicate standard error of mean. western blot analysis using anti-FLAG antibody was conducted to check the level of H-NS production under these conditions (Supplementary Figure S1A). (**B**) Phos-tag based western blot analysis showing the level of phosphorylated H-NS in the MR-1 H-NS^{FLAG} strain growing at two different temperate and during temperature shifts. The anti-FLAG was used as primary antibody to identify phosphorylated and nonphosphorylated H-NS protein. The phosphorylated H-NS is marked as H-NS-P and the nonphosphorylated is marked as H-NS. Regular western blot analysis without Phos-tag serves as control to show the total level of H-NS protein in each lane (~20 μg). The relative intensity of H-NS-P *vs* total H-NS (phosphorylated and nonphosphorylated) was quantified by ImageJ software. (**C**) Time course analysis of phosphorylated H-NS by Phos-tag based western blot analysis after temperature shift. Regular western blot analysis without Phos-tag serves as control to show the total level of H-NS protein in each lane (~20 μg). The relative intensity of H-NS-P versus total H-NS was quantified by ImageJ software. Experiments were performed with three independent cultures, and only representative images are presented here. Significant changes are marked with one asterisk for $P < 0.05$.

the H-NS protein consists of a C-terminal DNA-binding domain and a coiled-coil N-terminal domain that mediates oligomerization, similar to *E. coli*, *Salmonella* and *Vibrio* (28,47,48) (Figure 2). Specifically, we observed that all three phosphorylated residues are in the N-terminal oligomerization domain. Among these three residues, residue 2 is a highly conserved Ser, and residue 71 is either Ser or Asp (D). Notably, residue 42 is a conserved Glu (E) in *E. coli*, *Salmonella* and *Vibrio* but variable in *Shewanella* strains isolated from habitats with diverse ranges of temperatures. Most *Shewanella* strains have Ser at residue 42, but strains NCIMB400 (isolated from the North Sea) and BA175 (isolated from the Baltic Sea at a depth of 120 m) have Glu (E), and PV-4 (isolated from the deep sea in the Pacific ocean at a depth of 1325 m) has Lys (K) at residue 42. Since Glu (E) or Asp (D) is known to mimic a phosphorylated state of Ser, it appears that residue 42 of H-NS may behave as phosphorylated in some *Shewanella* strains (Figure 2).

Site-directed mutagenesis was employed to replace Ser with alanine (Ala, A) of H-NS to test which serine is phosphorylated in *S. oneidensis in vivo*. Ser differs from Ala in that one of the methylene hydrogen atoms is replaced by a hydroxyl group; thus, substitution of Ser by Ala prevents potential phosphorylation. H-NS with each of the three Ser residues mutated to Ala (A2, A42 or A71), as well as the WT (as control), was tagged in frame with FLAG using the pBBR1MCS-2 plasmid and expressed in the Δ*hns* strain using the native promoter of *hns* (Supplementary Table S1). Phos-tag was utilized to separate phosphorylated H-NS and nonphosphorylated H-NS by western blot. Notably, a nonphosphorylated protein band could only be seen when S42 was mutated to A42 at 30°C. These results indicate that phosphorylation of H-NS generally occurred at multiple serine sites at 30°C, but a fraction of H-NS proteins was only phosphorylated at S42 (Supplementary Figure S2B). As expected, the amount of nonphosphorylated H-NS protein of WT and the three variants were compara-

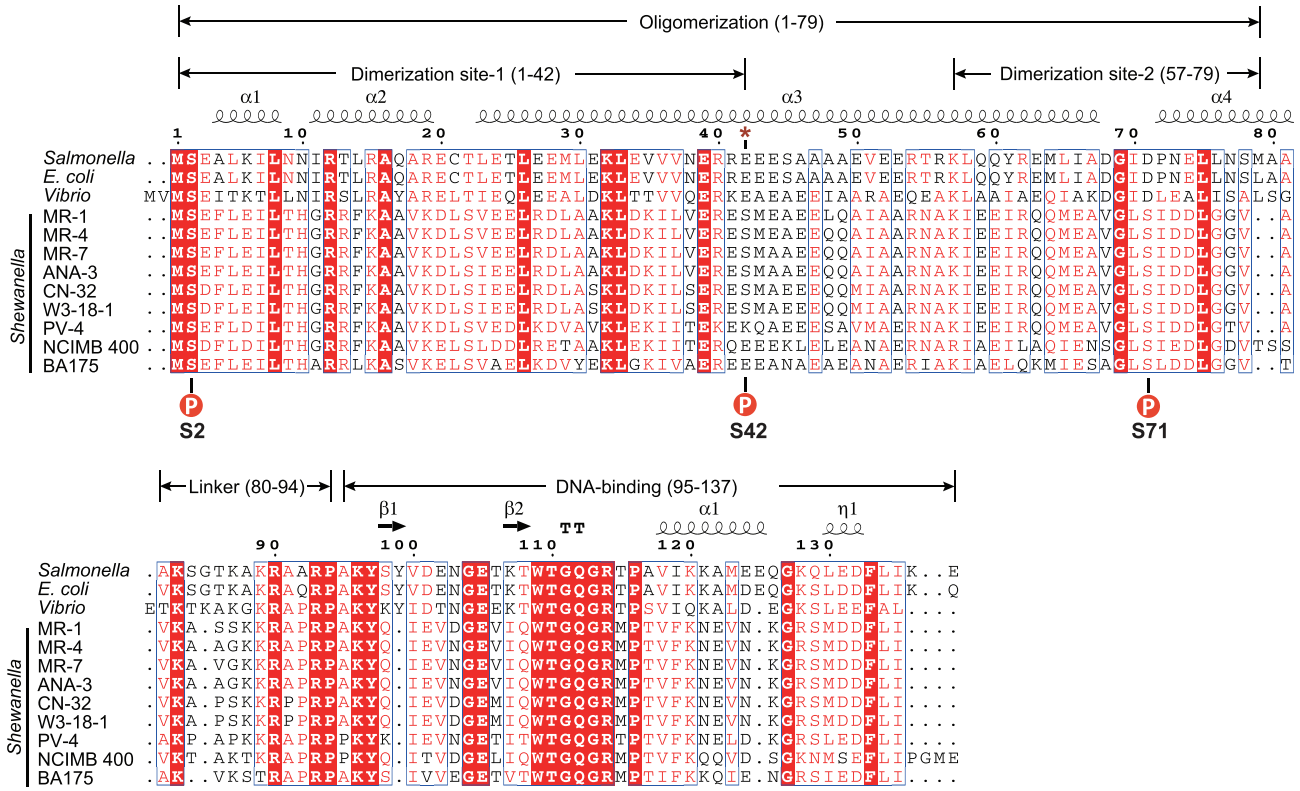

Figure 2. Phosphorylation sites of H-NS in *Shewanella*. Alignment of H-NS proteins from *Salmonella* (*S. enterica* serovar Typhimurium LT2), *E. coli* (*E. coli* K-12 MG1655), *Vibrio* (*Vibrio cholerae* O395) and nine *Shewanella* strains. The predicted secondary structure is shown on the top and the three identified phosphorylated serine residues are marked on the bottom. The nine *Shewanella* strains include *S. oneidensis* MR-1, *S.* sp. MR-4, *S.* sp. MR-7, *S.* sp. ANA-3, *S. putrefaciens* CN-32, *S. putrefaciens* W3–18-1, *S. loihica* PV-4, *S. frigidimarina* NCIMB 400 and *S. baltica* BA175.

ble when cells were cultured at 15°C (Supplementary Figure S2C).

Phosphorylation at S42 of H-NS is required for silencing prophage CP4So

To explore whether the phosphorylation of H-NS participates in prophage excision, two different types of site-directed mutagenesis were performed on the three Ser residues of H-NS (Figure 3A). As noted above, substitution of Ser by Ala mimics a nonphosphorylated state of the Ser residue. Conversely, substitution of Ser by Asp (D) mimics phosphorylation of the Ser residue. Next, we investigated whether these mutations affect the ability of H-NS to control prophage excision. The wild-type H-NS and its derived H-NS mutants were expressed via pBBR1MCS-2 under the *hns* promoter in the Δ*hns* strain to eliminate the effect of the chromosomal encoded H-NS. Among the four prophages in *S. oneidensis*, H-NS only regulates excision of prophage CP4So (11). Consistent with our previous finding, deletion of *hns* considerably increased CP4So prophage excision (∼1000-fold), and complementation by WT H-NS restored its original low level (∼1 out of 10^5 cells) at 30°C (Figure 3A). However, substitution of S42 by A42 completely abrogated the ability of H-NS to repress CP4So excision, while substitution of S42 by D42 did not affect the ability of H-NS to repress CP4So excision. Substitutions of S2 or S71 did not affect the ability of H-NS to control prophage excision. These results suggest that the phosphorylation of S42 is critical for the silencing of CP4So by H-NS.

We previously showed that H-NS silences CP4So excision by binding to the promoter of the prophage excisionase gene *alpA* (11). AlpA induces the genome excision of CP4So, thereby leading to the disruption of SsrA (small stable RNA A), and inactivation of *ssrA* decreases resistance to various stressors (34,49). Additionally, cell viability was greatly reduced when *alpA* was overexpressed in the WT and ΔCP4So strains at 30°C (Supplementary Figure S3AB). The toxic effect of AlpA is consistent with our earlier report on the prophage CP4–57 excisionase AlpA in *E. coli* (50). Therefore, the expression of *alpA* should be silenced or maintained at a low level at 30°C. As shown in Supplementary Figure S3C, two identical putative H-NS binding sites (5′-GATAATG-3′) are found in the promoter region of *alpA* (104 and 183 bp upstream of the start codon of *alpA*). This binding motif is highly similar to the consensus binding motif of H-NS in *E. coli* (51). The effect of H-NS phosphorylation on *alpA* was first explored *in vivo* by using a transcriptional *lacZ* fusion. In brief, the promoterless *lacZ* gene was fused with the promoter of *alpA* to make a P_{alpA}::*lacZ* fusion and cloned into plasmid pHGI01. The constructed plasmid was site-specifically integrated into the *nrfD* gene of the Δ*hns* strain, and *alpA* promoter activity was subsequently determined by measuring β-galactosidase activity. Consistent with the results of our previous study,

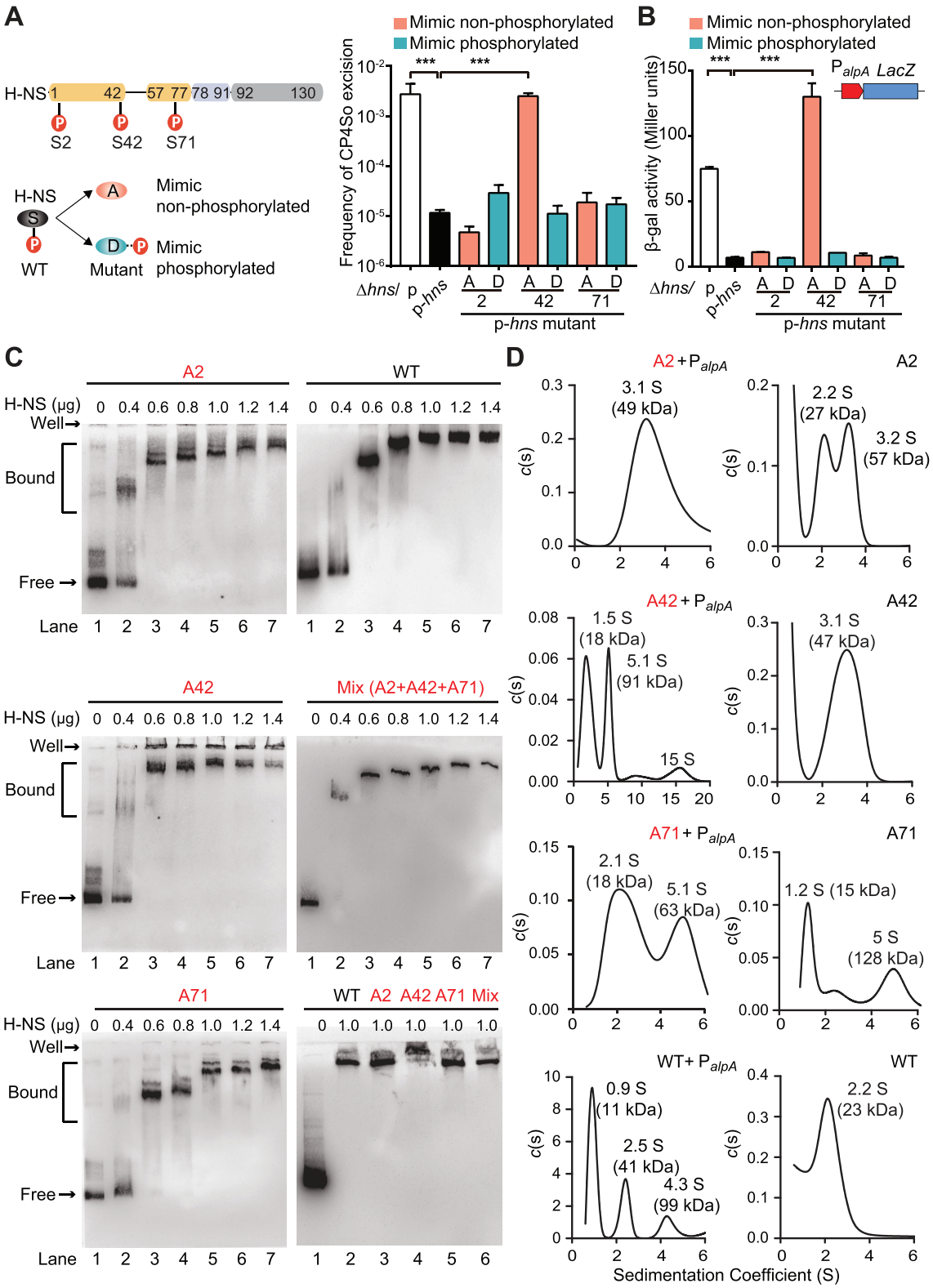

Figure 3. Phosphorylation of S42 is critical for silencing prophage. (**A**) Schematic representation of the aa substitutions of H-NS protein. The Ser (S) residue of H-NS was mutated to Ala (A) or Asp (D), respectively. Frequency of CP4So excision was quantified in Δ*hns* strain with H-NS variant produced via the pBBR1MCS-2 based plasmids. (**B**) Impact of phosphorylation/dephosphorylation of H-NS at S42 on the activity of the *alpA* promoter. The *lacZ* reporter system (P*alpA*::lacZ) was integrated into Δ*hns* strain. Cells grown to mid-log phase were harvested for the assays. (**C**) EMSA using purified WT H-NS, H-NS variants (A2, A42, A71) or a mixture of H-NS variants (three variants were added at an equal amount) purified at 30°C and the *alpA* promoter (0.5 pmol). (**D**) Sedimentation coefficient profiles of WT H-NS and three H-NS variants in the presence or absence of P*alpA*. Three independent cultures of each strain were tested and error bars indicate standard error of mean ($n = 3$) in (A) and (B). Significant changes are marked with one asterisk for $P < 0.05$ and three asterisks for $P < 0.01$.

deletion of *hns* induced *alpA* expression, and complementation with WT H-NS in the Δ*hns* host considerably repressed *alpA* expression at 30°C (Figure 3B). Notably, among the six H-NS substitutions, only the substitution of S42 by A42 abrogated the ability of H-NS to repress *alpA* expression, suggesting that S42 is important for H-NS to silence *alpA*.

To further investigate how phosphorylation affects the DNA binding ability of H-NS *in vitro*, three H-NS variants (A2, A42 and A71) purified from the Δ*hns* strain carrying pHGE-based plasmids at 30°C (Supplementary Figure S4) were utilized for EMSA. As shown in Figure 3C, a similar pattern was observed for WT, A2 and A71 with increasingly reduced mobility of the DNA-protein complexes with increasing protein concentrations from 0.4 to 1.4 μg/well (lanes 2–7), suggesting a concentration dependence of H-NS occupancy of multiple binding sites or H-NS oligomerization on the DNA substrate. Mixed A2, A42 and A71 also shifted the *alpA* promoter in a similar pattern to that of the WT H-NS with increasing protein concentrations. In contrast, A42 showed a maximal gel shift band with some protein-DNA complex stuck in the gel wells at concentrations of ≥0.6 μg/well (lanes 3–7) compared to WT H-NS or A2/A71 mutants. To further test whether the formation of trapped protein-DNA complex is specific to A42, equal amounts of H-NS protein (1.0 μg/well) were used for the binding reaction and were loaded onto one gel to minimize the possible effect of gel concentrations or running conditions. Consistently, trapped product was only seen for A42 (last panel). These EMSA assays suggested that phosphorylation of Ser42 is critical for the DNA binding or oligomerization of H-NS.

To further analyze the oligomerization of H-NS variants in the presence or absence of substrate DNA, the protein–DNA complex species were determined by sedimentation velocity experiment using analytical ultracentrifugation (Figure 3D). Results showed the WT-DNA complex formed by WT H-NS and P*alpA* showed three species at 0.9 S, 2.5 S and 4.3 S (Svedberg coefficient). A2–DNA complex only show one species at 3.1 S. A42–DNA complex showed a species at 5.1 S which was also observed in A71–DNA complex. Moreover, a species at 15 S with a massive molecular weight was only observed in A42–DNA sample, which may explain the trapped A42–DNA complex in the well in the EMSA experiments.

Phosphorylation affects the silencing of xenogeneic DNA by H-NS

To determine the physiological relevance of phosphorylating H-NS, two sets of RNA-seq experiments were performed. H-NS is known to be a global xenogeneic silencer; however, only a small number of genes (including *alpA*) are known to be regulated by H-NS in *S. oneidensis*. Thus, the first set of experiments (Set 1) attempted to identify genes/operons that are specifically silenced by H-NS at 30°C using the Δ*hns* and WT strains. Set 2 was performed to search for genes/operons that are affected by phosphorylating S42 of H-NS using the three strains in Figure 3A (Δ*hns*/p, Δ*hns*/p-*hns*, Δ*hns*/*p-hns*A42).

Using expression fold >2 as the cutoff, a total of 278 genes were found to be silenced by H-NS by comparing

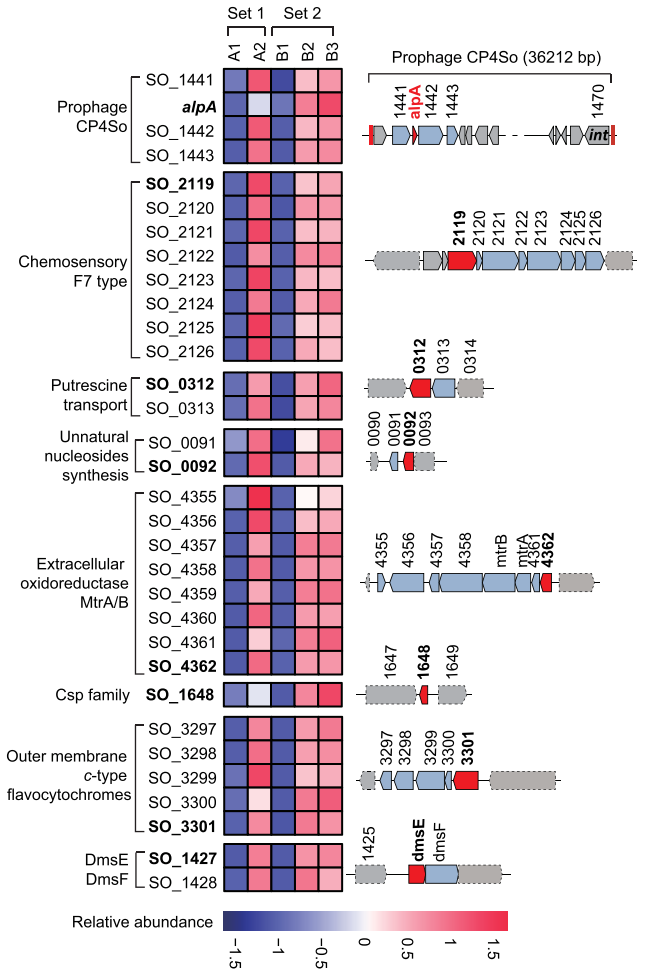

Figure 4. Heat map showing a subset of the 32 most highly upregulated genes by deleting *hns* gene (Set 1) and by mutating *hns* (from S42 to A42) (Set 2). RNA-seq were performed using Set 1 that includes two strains A1 (WT) and A2 (Δ*hns*) and Set 2 that includes three strains B1 (Δ*hns*/p-*hns*), B2 (Δ*hns*/p) and B3 (Δ*hns*/p-*hns*A42). Gene expression data normalized by *z*-score is shown on the left and the CP4So prophage and the six operons are shown on the right. Genes in bold fonts are the representative genes in each operon, which are further confirmed by qRT-PCR in Table 1.

the WT strain *versus* the Δ*hns* strain at 30°C in Set 1 (Supplementary File S2; Supplementary Figure S5). Repression of most of these genes (185 out of 278) by H-NS was further confirmed by using the Δ*hns*/p strain *versus* Δ*hns*/p-*hns* strain in Set 2 (Supplementary File S2; Supplementary Figure S5). More importantly, among the genes that were silenced by H-NS, we found that 179 genes were affected by the mutation of S42 to A42 in Set 2 (Supplementary File S2). Transcriptome profiles of the seven most highly regulated operons (including 32 genes) in the two sets of RNA-seq experiments are shown in Figure 4 and Supplementary Table S3, and comparative genome analysis suggests that they are laterally acquired (35). These genes/operons include those from prophage CP4So (SO_1441–1443, including *alpA*), a stress-related chemosensory system (SO_2119–2126) (52), the putrescine transport operon (SO_0312–0314), a cold shock family protein (CSP) SO_1648, and an operon that can synthesize unnatural nu-

Table 1. The signal (FPKM) of the eight most highly expressed genes/operons identified by RNA-seq of Set 1 and Set 2. Confirmation of the fold-change of RNA-seq was conducted by qRT-PCR for Set 2. FPKM, fragments per kilobase of transcript per million mapped reads.

Set	Set 1 FPKM		Set 2 FPKM			Set 2 qRT-PCR (Fold-change)	
Gene name	A1 WT	A2 Δ*hns*	B1(Δ*hns*/p- *hns*)	B2 (Δ*hns*/p)	B3 (Δ*hns*/p-*hns*A42)	B2 *vs* B1	B3 *vs* B1
SO_4821 (*alpA*)	0.1	15.56	1.92	34.51	42.21	10.9 ± 1.0	9.5 ± 1.0
SO_2119	4.29	163.98	1.69	98.88	111.42	12.1 ± 0.7	11.5 ± 0.8
SO_0312 (*porin*)	25.77	175.33	2.83	171.84	215.74	11.5 ± 0.7	10.6 ± 0.6
SO_1648 (*csp*)	33.26	78.92	12.98	135.64	172.44	11.0 ± 0.9	19.8 ± 0.9
SO_4362	2.69	72.89	4.42	59.24	59.77	17.7 ± 0.1	18.9 ± 0.1
SO_3301	5.06	48.01	2.54	51.46	46.07	14.7 ± 0.6	15.7 ± 0.6
SO_0092 (*deoD*)	2.99	24.58	1.72	17.54	16.8	5.9 ± 0.8	7.2 ± 0.9
SO_1427 (*dmsE*)	4.13	26.77	4.13	24.55	25.74	4.2 ± 0.8	5.0 ± 0.6
SO_3146 (*hns*)	629.08	0.001	4255.18	4.01	3030.71	-	-

cleosides (SO_0091–0092). Additionally, three operons related to the extracellular electron transfer (EET) pathways include the periplasmic electron transfer via the periplasmic decaheme *c*-type cytochromes (SO_4355–4362), including MtrA and MtrB, an outer membrane flavocytochrome *c* flavin subunit (SO_3297–3301), and DmsE and DmsF (SO_1427–1428). Similar patterns were found comparing the Δ*hns* strain and WT strain in Set 1 and comparing WT and alanine mutation at 42 position mutated H-NS (A42) in the absence of a chromosomal copy of H-NS in Set 2, suggesting that the silencing of these laterally acquired genes requires phosphorylation of H-NS at Ser42.

To verify the RNA-seq results of Set 2, seven representative genes in seven operons and SO_1648 were selected and tested by qRT-PCR analysis (Table 1). Notably, the expression levels of these genes were very low in the WT or Δ*hns*/pH-NS strains, indicating that these genes are silenced at 30°C by H-NS. Consistent with the RNA-seq results, both *hns* deletion and alanine mutation at 42 (A42) activated the expression of these genes, suggesting that S42 needs to be phosphorylated for H-NS to serve as a xenogeneic silencer for these genes. Additionally, transcription of 93 genes was increased in the Δ*hns* strain, but the expression of these genes was not affected by mutating S42 (Supplementary File S2), suggesting that another mechanism may govern their selective silencing by H-NS under different conditions.

Silencing of two cold inducible genes also requires phosphorylation of H-NS at S42

Since H-NS is nonphosphorylated at cold temperatures, we investigated whether the genes repressed by phosphorylated H-NS are also induced at cold temperatures, similar to *alpA*. To test this hypothesis, the change in the expression level of these genes in Table 1 was quantified by qRT-PCR in the WT cells 2 h after the temperature downshift from 30 to 15°C. Among eight representative genes, SO_1648 was the most highly induced (16.72-fold) by the temperature reduction Figure 5A. There are five CSPs (SO_0733, SO_1648, SO_1732, SO_2628, SO_2787) in *S. oneidensis*; SO_1648 displayed some sequence identity to *E. coli* CspA (∼66%). Notably, previous whole-genome DNA microarrays used to investigate temporal gene expression profiles in *S. oneidensis* in response to a temperature downshift demonstrated that SO_1648 was highly upregulated and induced 14-fold after a downshift from 30 to 8°C (53). Additionally, phenotypic analyses demonstrated that SO_1648 was the only functional CSP protein at cold temperatures upon deleting each of the 5 CSP genes (53). Temperature downshift also resulted in a 9.16-fold increase in *alpA* expression and a 9.67-fold increase in SO_2119 expression (Figure 5A). Although the exact function of SO_2119 is not known, overexpression of SO_2119 results in growth inhibition of *S. oneidensis* at 30°C (Supplementary Figure S6A). The expression of SO_2119 was found to be silenced at 30°C by H-NS (Table 1). Putative A/T-rich H-NS binding sites were found in the promoter regions of SO_1648 and SO_2119 (Supplementary Figure S6B). EMSA was performed using the promoter region of SO_1648 or SO_2119 and showed that A42 still appeared to aggregate more easily when it was binding to these promoters compared to the WT H-NS and other H-NS variants purified from 30°C (Figure 5B). The mixed H-NS variants showed a similar binding profile as the WT H-NS. These results are consistent with the binding of H-NS WT and variants to the *alpA* promoter (Figure 3C), suggesting that S42 is important for H-NS to silence these genes at 30°C.

Furthermore, we purified the H-NS protein at 15°C, and EMSA was conducted to compare the binding of H-NS from two different temperatures to the same promoter region. Compared to the H-NS protein from 30°C, the H-NS protein purified from 15°C exhibited reduced binding activity to the promoter region of *alpA*, SO_1648 or SO_2119 at lower protein concentrations (<1.0 μg/well in Supplementary Figure S6C), while it formed a similar aggregated complex with these promoters at a higher protein concentration (>1.0 μg/well in Figure 5C). This result indicates that the nonphosphorylated H-NS has a reduced ability to repress the expression of these cold-inducible genes at 15°C. Moreover, qRT-PCR was employed to quantify the expression of the three cold-inducible genes at 30 and 15°C. In keeping with the previous results, mutating S42 to A42 greatly reduced the ability of H-NS to repress the expression of these genes at 30°C (Figure 5D), but no effect was observed at 15°C (Supplementary Figure S7). Mutating S42 to D42 showed a reduced ability to repress *alpA* and SO_2119 than the WT H-NS at 30°C, indicating that H-NS with S42 exerts stronger repression than H-NS with D42 in which H-NS is in permanently phosphorylated state at this residue. Mutating S71 to A71 slightly reduced the ability of H-NS to repress the expression of SO_2119 at 30°C, suggesting that

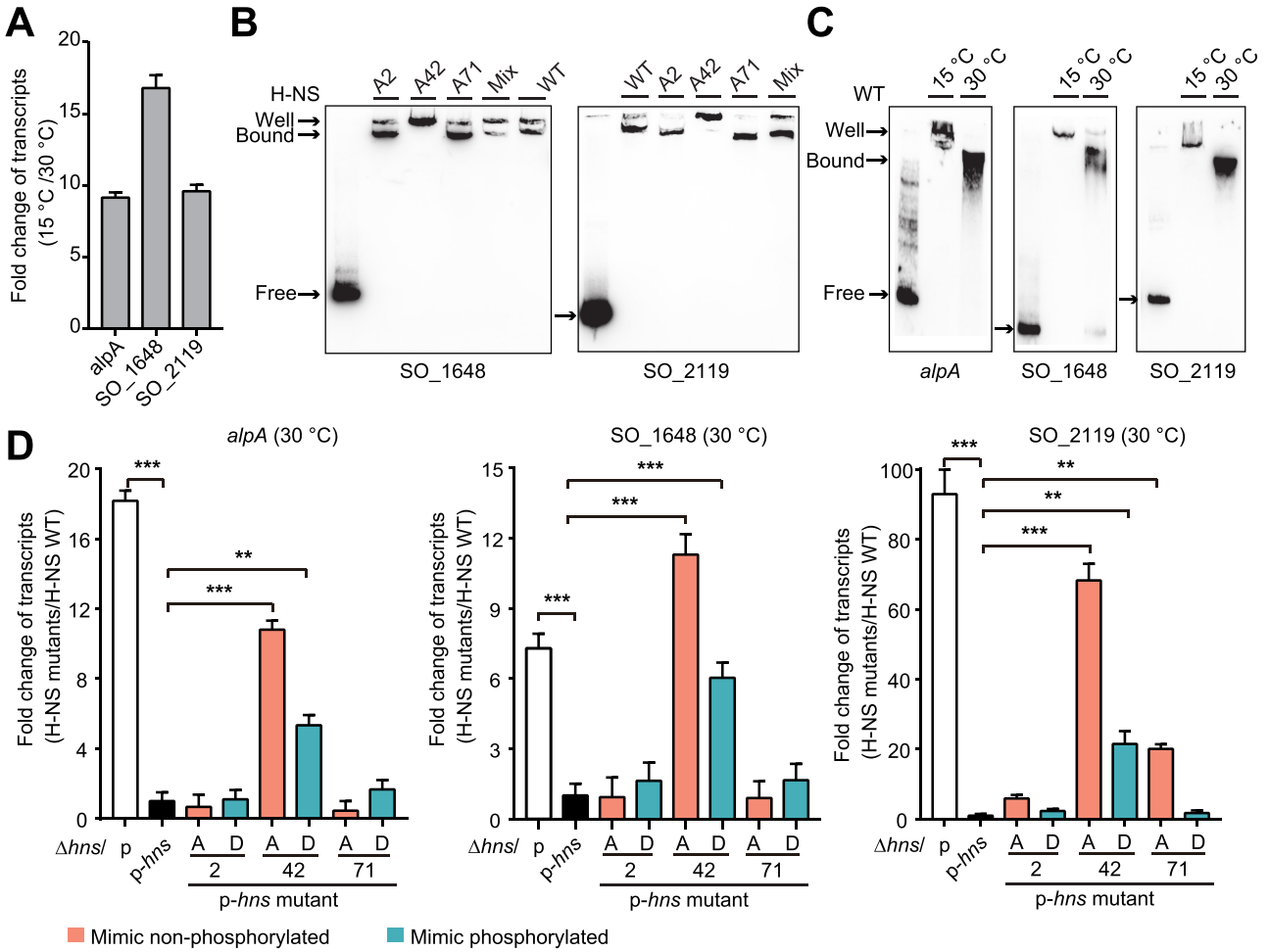

Figure 5. Phosphorylation of S42 is critical for silencing cold inducible genes. (**A**) Fold-change of transcripts of three genes (15°C versus 30°C) quantified by qRT-PCR. Data are from three independent cultures and one standard deviation is shown. (**B**) EMSA using H-NS variants (A2, A42, A71) and WT H-NS purified from plasmid carrying Δ*hns* cultured at 30°C. For the mixture, equal amount of three H-NS variants were used and the final total amounts of protein were indicated. (**C**) EMSA using WT H-NS purified from Δ*hns* cultured at 15°C. (**D**) Impact of phosphorylation/dephosphorylation of H-NS at S2, S42 and S71 on the transcriptional change of *alpA*, SO_1648 or SO_2119. Expression of the 16S ribosomal RNA gene *rrsE* was used to normalize the total RNA in different samples in (A) and (D). Three independent cultures of each strain were tested and error bars indicate standard error of mean ($n = 3$). Significant changes are marked with one asterisk for $P < 0.05$ and three asterisks for $P < 0.01$.

phosphorylation of the A71 might also be involved in the selective silencing of H-NS.

Putative Ser/Thr kinases and phosphatases in *S. oneidensis*

There are two possible explanations for the decreasing level of phosphorylated H-NS after temperature downshifts: reduced kinase activity to act on newly synthesized protein or increased phosphatase activity to dephosphorylate existing protein. We then searched for putative kinases and phosphatases that use Ser/Thr as substrates in the genome of *S. oneidensis*. Three genes were found to encode putative Ser/Thr phosphatases (Supplementary Table S4). SerB (SO_1223) catalyzes the last step in L-serine biosynthesis and CheZ (SO_3208) participates in the chemotaxis signal transduction pathway by dephosphorylation-free CheY (54,55) and therefore these would not be expected to act on H-NS. The third, SO_2119, is a hypothetical protein with some sequence identity (28%) with the phosphatase SpoIIE of *Bacillus subtilis,* which is conserved in eukaryotes and prokaryotes (56,57) (Supplementary Table S4). To determine whether SO_2119 plays a role in the dephosphorylation of H-NS, western blot analysis using Phos-tag and anti-FLAG antibodies was performed on MR-1 H-NS^{FLAG} cells with SO_2119 deleted. At both 30 and 15°C, the level of phosphorylated H-NS was the same in the presence or the absence of SO_2119, suggesting that H-NS is not the target of SO_2119 (Supplementary Figure S8A).

Eight genes encoding putative Ser/Thr protein kinases were found (Supplementary Table S5). Among these genes, SO_1461 encodes a eukaryotic-type Ser/Thr kinase of the PknB subfamily that was recently shown to phosphorylate the H-NS analog Lsr2 in *Mycobacterium tuberculosis* and is located inside CP4So (Supplementary Figure S8B). The PknB subfamily of Ser/Thr kinases includes *Staphylococcus aureus* PknB, *Bacillus subtilis* PrkC, and *M. tuberculosis* Pkn proteins. The previously characterized PknB members contain an N-terminal cytosolic kinase do-

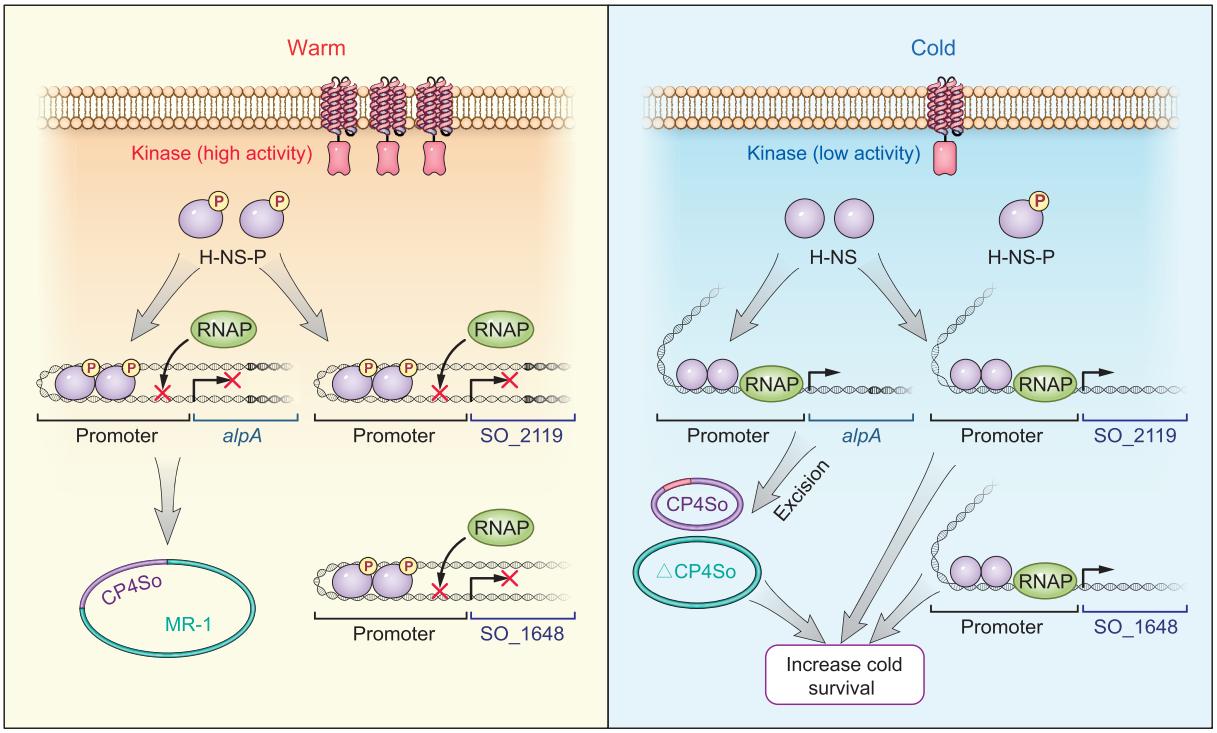

Figure 6. A proposed mechanism of xenogeneic silencing by H-NS. At warm temperatures, host H-NS is phosphorylated by the serine kinase and the phosphorylated H-NS binds to the promoter region of the xenogeneic genes (e.g. *alpA*, SO_2119 or SO_1648) to silence them. Thus, prophage CP4So is stably maintained in the host genome and SO_2119 and SO_1648 are not produced to minimize host burden. At cold temperatures, the activity of kinase is reduced and newly synthesized H-NS is no longer phosphorylated. Non- phosphorylated H-NS de-represses the promoter and induces the expression of these genes. As a result, CP4So is excised and SO_1648 is produced, thereby increasing host fitness in the cold.

main, a transmembrane segment, and multiple C-terminal extracellular PASTA domains that are thought to bind beta-lactam compounds and peptidoglycans (Supplementary Figure S8B). Blast research demonstrated that the N-terminus of SO_1641 contains a putative ATP binding domain and a transmembrane domain (Supplementary Figure S8C), but the overall identification with known PknB is less than 30%. Thus, we investigated whether SO_1461 can phosphorylate H-NS. Western blot analysis using Phos-tag and anti-FLAG antibodies was performed with MR-1 H-NS^{FLAG} cells overexpressing SO_1461 at 15°C, and the level of phosphorylated H-NS was increased with the expression of SO_1461 (Supplementary Figure S8D).

Homologs of SO_1461 that share medium to high amino acid identity (~40–90%) are present in several *Proteus*, *Vibrio*, *Pseudomonas* and *Xanthomonas* strains (Supplementary Figure S8B), and these homologs are all putative kinases. Notably, unlike the PknB found in Gram-positive bacteria, the *pknB*-like genes are in mobile elements, such as integrative and conjugative elements (ICEs) or prophages, suggesting that they are acquired horizontally. However, several attempts to delete SO_1461 were made at 30°C, but no deletion mutant was obtained, presumably because the gene may be essential in the presence of prophage CP4So. This result is consistent with the findings of earlier reports, which showed that the PknB was essential in *M. tuberculosis* (58) and that *pknB* can only be deleted in osmoprotective sucrose magnesium medium (59).

DISCUSSION

Many bacteria, such as *Shewanella,* must withstand a wide range of temperature shifts daily or seasonally. For these bacteria, activating or silencing genes at different temperatures is critical. In this study, we demonstrate a new method of decision-making for xenogeneic silencing via temperature-dependent posttranslational modification of the host H-NS protein (Figure 6). Specifically, host H-NS is modulated by a serine kinase via phosphorylation to gain control of LGT genes in response to temperature changes. At warmer temperatures where planktonic growth is preferred, phosphorylated H-NS prophage silencing of the phage excisionase genes *alpA* and CP4So is maintained in a lysogenic state. Additionally, genes in the extracellular electron transfer pathways, a cold shock protein, and a stress-related chemosensory system are also all silenced by phosphorylated H-NS at warm temperatures. When temperature decrease, H-NS proteins become increasingly nonphosphorylated due to reduced kinase activity, and nonphosphorylated H-NS no longer represses these LGT genes. As a result, the CP4So prophage is excised, and the transcription of SO_1648 is activated at cold temperatures to promote host fitness. Additionally, the CP4So-encoded PknB homolog SO_1461 can phosphorylate H-NS when overproduced. This result exemplifies a symbiotic relationship between the LGT genes (including phage) and bacterial host protein when the interests of both sides are aligned to react and thrive in variable environmental conditions.

Silencing foreign DNAs with preferences for AT-rich regions is an important function of H-NS, and the alleviation of xenogeneic silencing by H-NS also requires tight control. Previously, we found that among the four prophages in *S. oneidensis*, H-NS only silences CP4So, the only prophage that is excised during the temperature reduction, and this process is important for host cold adaptation (11). Among the five CSPs in *S. oneidensis*, SO_1648 is among the most highly induced genes during the temperature downshift from 30 to 8°C by whole-genome microarray analysis, and mutational analyses confirmed that SO_1648 is the only functional Csp protein at very low temperatures (53). Notably, we found that SO_1648 is the only Csp protein that is silenced by phosphorylated H-NS at 30°C. Dephosphorylation of H-NS affects the expression of SO_1648. These results indicate that the genes/operons that are silenced by H-NS at warm temperatures and derepressed at cold temperatures are important for the survival of *S. oneidensis* in the cold. Furthermore, the genes that are involved in extracellular electron transfer pathways are also silenced by phosphorylated H-NS. It makes sense for these genes to be silenced during aerobic respiration. The ability of oxidizing insoluble metals to be utilized as external electron acceptors for anaerobic respiration might also be important in the cold adaptation of *S. oneidensis* in specific niches, especially because a temperature decrease also leads to a reduced solubility of several metals. Moreover, the promoter regions of these genes containing two or more predicted H-NS binding motifs are all more AT-rich (AT content $\geq$ 63.2%) (Supplementary Figures S3A and 6B) than the average AT contents of *S. oneidensis* MR-1 genome (54.1%). In several bacterial pathogens, H-NS or H-NS homologs control the temperature-dependent induction of virulence factors, including *pap* (pyelonephritis-associated pili) and *fimA* (fimbrilin A) in *E. coli* (18,60) and *virF* (virulence factor F) in *Shigella flexneri* (61). It has not been determined whether a temperature-dependent posttranslational modification plays a role in the regulation of these virulence operons by H-NS or H-NS homologs.

Recently, the importance of posttranslational modification of nucleoid-associated proteins in different bacteria has been reviewed (62). Several recent studies have examined the changes in the regulatory role of H-NS due to posttranslational modification (59,63). One study used proteomic analysis and found that phosphorylation of H-NS on Thr13 is important for upregulation of a wide range of genetic loci, including the PhoP/PhoQ-regulated genes in *Salmonella enterica* serovar Typhimurium (63). Another study found four phosphorylated Thr residues of the H-NS analog in *M. tuberculosis,* and phosphorylation of Thr112 is required for *M. tuberculosis* to grow on solid media and to survive under hypoxic conditions (59). A recent study reported that the expression of foreign genes of *Salmonella* is activated inside macrophages through degradation of H-NS by the protease Lon (64). Our study provides direct evidence that posttranslational modification of H-NS involving serine is critical in the thermoregulation of H-NS. Additionally, we observed that the phosphorylation of Ser42 is critical for H-NS to silence the expression of several LGT genes. The ability to multimerize is important for H-NS in gene silencing (65–67), and changes in temperature affect the capacity of H-NS to form multimers that condense DNA and repress gene expression (26,28). Biophysical studies have demonstrated that an increase in temperature promotes a conformational change in the dimerization site (25,28). A total of three phosphorylated residues are located within the oligomerization domain of H-NS, and phosphorylation of Ser42 is found to be most important for xenogeneic silencing of the genes that are induced at low temperatures. We noticed that mutating Ser to Asp/Glu showed reduced abilities to repress *alpA* and SO_2119 than the WT H-NS at 30°C. In *E. coli*, H-NS can bind to its protein partner such as Hha or StpA to form heteromultimer to control its target genes (68). It is possible that changing Ser42 into a permanently phosphorylated residual such as Asp/Glu may affect the binding of H-NS to its protein partner in *S. oneidensis*. Further biophysical studies and structural analyses are warranted to explore how the conformational change upon the phosphorylation of various residues of H-NS affects the DNA binding of H-NS.

Protein phosphorylation mediated by Ser/Thr protein kinases is widely utilized to transduce extracellular signals into intracellular responses. Compared to the Ser/Thr protein kinases in eukaryotes, the control mechanisms of these kinases are less well understood in prokaryotes. Furthermore, previous studies primarily focused on Gram-positive bacteria, including *M. tuberculosis, S. aureus* or *Listeria monocytogenes*. Among these bacteria, PknB is an essential membrane protein in *M. tuberculosis* (58), and it plays a key role in regulating growth, cell division and envelope synthesis in *M. tuberculosis or S. aureus* (69,70). Notably, an H-NS analog Lsr2 protein in *M. tuberculosis* is phosphorylated by PknB *in vitro* (59). In this study, we found a PknB homolog inside the CP4So prophage, but it exhibits low sequence similarity with PknB of Gram-positive bacteria. The PknB proteins of Gram-negative bacteria, such as *S. oneidensis*, *P. mirabilis* and *Vibrio*, are highly conserved and are considerably larger than those of Gram-positive bacteria (1376 aa in *S. oneidensis versus* 626 aa in *M. tuberculosis*), possessing a long and different C-terminus with no predicted function. Notably, in many Gram-negative bacteria, these kinases are within mobile genetic elements and in proximity to a restriction-modification system. It remains to be explored whether these kinases can rewire the host protein and are involved in the silencing of these mobile elements.

SUPPLEMENTARY DATA

Supplementary Data are available at NAR Online.

ACKNOWLEDGEMENTS

We are grateful to Dr Haichun Gao from Zhejiang University for providing us with plasmids of pHGM01 and pHGEI01. We thank Dr Xilin Zhao from Rutgers University, Dr Jun Zhu from University of Pennsylvania, Dr Hongbo Luo from Harvard Medical School for their inspiring discussions, and Drs Shaowei Li and Tingting Li from Xiamen University for help in the analytical centrifugation experiment.

Author contributions: X.L. and X.W. designed the study. X.L., S.L., T.L., Y.Z., W.W. and R.C. performed the experi-

ments. J.Y., Y.G. and K.T. contributed to the method development. X.W., X.L., J.Y., Y.G., K.T. and R.C. analyzed the data. X.W. and X.L. wrote the manuscript, and M.B. helped revise the manuscript. All of the authors read and approved the final manuscript.

FUNDING

National Key Research and Development Program of China [2018YFC1406500, 2017YFC0506303]; National Science Foundation of China [91951203, 31625001]; Guangdong Local Innovation Team Program [2019BT02Y262]; Key Special Project for Introduced Talents Team of Southern Marine Science and Engineering Guangdong laboratory (Guangzhou) [GML2019ZD0407]; Natural Science Foundation of Guangdong Province, China [2017A030313193]; K. C. Wong Education Foundation. Funding for open access charge: National Science Foundation of China.
Conflict of interest statement. None declared.

REFERENCES

1. Pfeifer,E., Hunnefeld,M., Popa,O. and Frunzke,J. (2019) Impact of xenogeneic silencing on phage-host interactions. *J. Mol. Biol.*, **431**, 4670–4683.
2. Singh,K., Milstein,J.N. and Navarre,W.W. (2016) Xenogeneic silencing and its impact on bacterial genomes. *Annu. Rev. Microbiol.*, **70**, 199–213.
3. Dorman,C.J. (2007) H-NS, the genome sentinel. *Nat. Rev. Microbiol.*, **5**, 157–161.
4. Navarre,W.W., Porwollik,S., Wang,Y., McClelland,M., Rosen,H., Libby,S.J. and Fang,F.C. (2006) Selective silencing of foreign DNA with low GC content by the H-NS protein in *Salmonella*. *Science*, **313**, 236–238.
5. Lucchini,S., Rowley,G., Goldberg,M.D., Hurd,D., Harrison,M. and Hinton,J.C. (2006) H-NS mediates the silencing of laterally acquired genes in bacteria. *PLoS Pathog.*, **2**, e81.
6. Will,W.R., Navarre,W.W. and Fang,F.C. (2015) Integrated circuits: how transcriptional silencing and counter-silencing facilitate bacterial evolution. *Curr. Opin. Microbiol.*, **23**, 8–13.
7. Liu,X., Li,Y., Guo,Y., Zeng,Z., Li,B., Wood,T.K., Cai,X. and Wang,X. (2015) Physiological function of rac prophage during biofilm formation and regulation of rac excision in *Escherichia coli* K-12. *Sci. Rep.*, **5**, 16074.
8. Castang,S. and Dove,S.L. (2012) Basis for the essentiality of H-NS family members in *Pseudomonas aeruginosa*. *J. Bacteriol.*, **194**, 5101–5109.
9. Li,C., Wally,H., Miller,S.J. and Lu,C.-D. (2009) The multifaceted proteins MvaT and MvaU, members of the H-NS family, control arginine metabolism, pyocyanin synthesis, and prophage activation in *Pseudomonas aeruginosa* PAO1. *J. Bacteriol.*, **191**, 6211–6218.
10. Li,Y., Liu,X., Tang,K., Wang,P., Zeng,Z., Guo,Y. and Wang,X. (2019) Excisionase in Pf filamentous prophage controls lysis-lysogeny decision-making in *Pseudomonas aeruginosa*. *Mol. Microbiol.*, **111**, 495–513.
11. Zeng,Z., Liu,X., Yao,J., Guo,Y., Li,B., Li,Y., Jiao,N. and Wang,X. (2016) Cold adaptation regulated by cryptic prophage excision in *Shewanella oneidensis*. *ISME J.*, **10**, 2787–2800.
12. Rodrigues,D.F. and Tiedje,J.M. (2008) Coping with our cold planet. *Appl. Environ. Microbiol.*, **74**, 1677–1686.
13. Shivaji,S. and Prakash,J.S.S. (2010) How do bacteria sense and respond to low temperature? *Arch. Microbiol.*, **192**, 85–95.
14. Gualerzi,C.O., Maria Giuliodori,A. and Pon,C.L. (2003) Transcriptional and post-transcriptional control of cold-shock genes. *J. Mol. Biol.*, **331**, 527–539.
15. Barria,C., Malecki,M. and Arraiano,C.M. (2013) Bacterial adaptation to cold. *Microbiology*, **159**, 2437–2443.
16. Dorman,C.J. (2004) H-NS: a universal regulator for a dynamic genome. *Nat. Rev. Microbiol.*, **2**, 391–400.
17. Pon,C.L., Calogero,R.A. and Gualerzi,C.O. (1988) Identification, cloning, nucleotide sequence and chromosomal map location of *hns*, the structural gene for *Escherichia coli* DNA-binding protein H-NS. *Mol. Gen. Genet.*, **212**, 199–202.
18. Goransson,M., Sonden,B., Nilsson,P., Dagberg,B., Forsman,K., Emanuelsson,K. and Uhlin,B.E. (1990) Transcriptional silencing and thermoregulation of gene expression in *Escherichia coli*. *Nature*, **344**, 682–685.
19. Atlung,T. and Ingmer,H. (1997) H-NS: A modulator of environmentally regulated gene expression. *Mol. Microbiol.*, **24**, 7–17.
20. Hommais,F., Krin,E., Laurent-Winter,C., Soutourina,O., Malpertuy,A., Le Caer,J.P., Danchin,A. and Bertin,P. (2001) Large-scale monitoring of pleiotropic regulation of gene expression by the prokaryotic nucleoid-associated protein, H-NS. *Mol. Microbiol.*, **40**, 20–36.
21. Ono,S., Goldberg,M.D., Olsson,T., Esposito,D., Hinton,J.C.D. and Ladbury,J.E. (2005) H-NS is a part of a thermally controlled mechanism for bacterial gene regulation. *Biochem. J.*, **391**, 203–213.
22. White-Ziegler,C.A. and Davis,T.R. (2009) Genome-wide identification of H-NS-controlled, temperature-regulated genes in *Escherichia coli* K-12. *J. Bacteriol.*, **191**, 1106–1110.
23. Eriksson,S., Hurme,R. and Rhen,M. (2002) Low-temperature sensors in bacteria. *Philos. Trans. R. Soc. Lond., B, Biol. Sci.*, **357**, 887–893.
24. Steinmann,R. and Dersch,P. (2012) Thermosensing to adjust bacterial virulence in a fluctuating environment. *Future Microbiol.*, **8**, 85–105.
25. Shahul Hameed,U.F., Liao,C., Radhakrishnan,A.K., Huser,F., Aljedani,S.S., Zhao,X., Momin,A.A., Melo,F.A., Guo,X., Brooks,C. *et al.* (2018) H-NS uses an autoinhibitory conformational switch for environment-controlled gene silencing. *Nucleic Acids Res.*, **47**, 2666–2680.
26. Bouffartigues,E., Buckle,M., Badaut,C., Travers,A. and Rimsky,S. (2007) H-NS cooperative binding to high-affinity sites in a regulatory element results in transcriptional silencing. *Nat. Struct. Mol. Biol.*, **14**, 441–448.
27. Grainger,D.C. (2016) Structure and function of bacterial H-NS protein. *Biochem. Soc. Trans.*, **44**, 1561–1569.
28. Arold,S.T., Leonard,P.G., Parkinson,G.N. and Ladbury,J.E. (2010) H-NS forms a superhelical protein scaffold for DNA condensation. *Proc. Natl. Acad. Sci. U.S.A.*, **107**, 15728–15732.
29. Marsili,E., Baron,D.B., Shikhare,I.D., Coursolle,D., Gralnick,J.A. and Bond,D.R. (2008) *Shewanella* secretes flavins that mediate extracellular electron transfer. *Proc. Natl. Acad. Sci. U.S.A.*, **105**, 3968–3973.
30. Hau,H.H. and Gralnick,J.A. (2007) Ecology and biotechnology of the genus *Shewanella*. *Annu. Rev. Microbiol.*, **61**, 237–258.
31. Fredrickson,J.K., Romine,M.F., Beliaev,A.S., Auchtung,J.M., Driscoll,M.E., Gardner,T.S., Nealson,K.H., Osterman,A.L., Pinchuk,G., Reed,J.L. *et al.* (2008) Towards environmental systems biology of *Shewanella*. *Nat. Rev. Microbiol.*, **6**, 592–603.
32. Caro-Quintero,A., Deng,J., Auchtung,J., Brettar,I., Hofle,M.G., Klappenbach,J. and Konstantinidis,K.T. (2011) Unprecedented levels of horizontal gene transfer among spatially co-occurring*Shewanella* bacteria from the Baltic Sea. *The ISME J.*, **5**, 131–140.
33. Konstantinidis,K.T., Serres,M.H., Romine,M.F., Rodrigues,J.L., Auchtung,J., McCue,L.A., Lipton,M.S., Obraztsova,A., Giometti,C.S., Nealson,K.H. *et al.* (2009) Comparative systems biology across an evolutionary gradient within the *Shewanella* genus. *Proc. Natl. Acad. Sci. U.S.A.*, **106**, 15909–15914.
34. Liu,X., Tang,K., Zhang,D., Li,Y., Liu,Z., Yao,J., Wood,T.K. and Wang,X. (2019) Symbiosis of a P2-family phage and deep-sea *Shewanella putrefaciens*. *Environ. Microbiol.*, **21**, 4212–4232.
35. Rodrigues,J.L., Serres,M.H. and Tiedje,J.M. (2011) Large-scale comparative phenotypic and genomic analyses reveal ecological preferences of *Shewanella* species and identify metabolic pathways conserved at the genus level. *Appl. Environ. Microbiol.*, **77**, 5352–5360.
36. Zhong,C.F., Han,M.Z., Yu,S.J., Yang,P.S., Li,H.J. and Ning,K. (2018) Pan-genome analyses of 24 *Shewanella* strains re-emphasize the diversification of their functions yet evolutionary dynamics of metal-reducing pathway. *Biotechnol. Biofuels*, **11**, 193.
37. Six,E.W. and Klug,C.A.C. (1973) Bacteriophage P4: satellite virus depending on a helper such as prophage P2. *Virology*, **51**, 327–344.
38. Yao,J., Guo,Y., Wang,P., Zeng,Z., Li,B., Tang,K., Liu,X. and Wang,X. (2018) Type II toxin/antitoxin system $ParE_{SO}/CopA_{SO}$

stabilizes prophage CP4So in *Shewanella oneidensis*. *Environ. Microbiol.*, **20**, 1224–1239.
39. Jian,H., Xu,G., Wang,F. and Xiao,X. (2017) Characterisation of the regulatory function of the H-NS protein in the benthic bacterium *Shewanella piezotolerans* WP3 under cold conditions. *FEMS Microbiol. Lett.*, **364**, doi:10.1093/femsle/fnx1021.
40. Fu,H., Jin,M., Ju,L., Mao,Y. and Gao,H. (2014) Evidence for function overlapping of CymA and the cytochrome bc1 complex in the *Shewanella oneidensis* nitrate and nitrite respiration. *Environ. Microbiol.*, **16**, 3181–3195.
41. Wang,X., Kim,Y., Ma,Q., Hong,S.H., Pokusaeva,K., Sturino,J.M. and Wood,T.K. (2010) Cryptic prophages help bacteria cope with adverse environments. *Nat. Commun.*, **1**, 147.
42. Pfaffl,M.W. (2001) A new mathematical model for relative quantification in real-time RT-PCR. *Nucleic Acids Res.*, **29**, e45.
43. Jin,M., Jiang,Y., Sun,L., Yin,J., Fu,H., Wu,G. and Gao,H. (2013) Unique organizational and functional features of the cytochrome c maturation system in *Shewanella oneidensis*. *PLoS One*, **8**, e75610.
44. Tan,M., Luo,H., Lee,S., Jin,F., Yang,J.S., Montellier,E., Buchou,T., Cheng,Z., Rousseaux,S., Rajagopal,N. *et al.* (2011) Identification of 67 histone marks and histone lysine crotonylation as a new type of histone modification. *Cell*, **146**, 1016–1028.
45. Kinoshita,E., Kinoshita-Kikuta,E., Takiyama,K. and Koike,T. (2006) Phosphate-binding tag, a new tool to visualize phosphorylated proteins. *Mol. Cell. Proteomics*, **5**, 749–757.
46. Schuck,P. (2000) Size-distribution analysis of macromolecules by sedimentation velocity ultracentrifugation and lamm equation modeling. *Biophys. J.*, **78**, 1606–1619.
47. Cerdan,R., Bloch,V., Yang,Y., Bertin,P., Dumas,C., Rimsky,S., Kochoyan,M. and Arold,S.T. (2003) Crystal structure of the N-terminal dimerisation domain of VicH, the H-NS-like protein of *Vibrio cholerae*. *J. Mol. Biol.*, **334**, 179–185.
48. Bloch,V., Yang,Y.S., Margeat,E., Chavanieu,A., Auge,M.T., Robert,B., Arold,S., Rimsky,S. and Kochoyan,M. (2003) The H-NS dimerization domain defines a new fold contributing to DNA recognition. *Nat. Struct. Biol.*, **10**, 212–218.
49. Muto,A., Fujihara,A., Ito,K.I., Matsuno,J., Ushida,C. and Himeno,H. (2000) Requirement of transfer-messenger RNA for the growth of *Bacillus subtilis* under stresses. *Genes Cells*, **5**, 627–635.
50. Wang,X., Kim,Y. and Wood,T.K. (2009) Control and benefits of CP4-57 prophage excision in*Escherichia coli* biofilms. *ISME J.*, **3**, 1164–1179.
51. Lang,B., Blot,N., Bouffartigues,E., Buckle,M., Geertz,M., Gualerzi,C.O., Mavathur,R., Muskhelishvili,G., Pon,C.L., Rimsky,S. *et al.* (2007) High-affinity DNA binding sites for H-NS provide a molecular basis for selective silencing within proteobacterial genomes. *Nucleic Acids Res.*, **35**, 6330–6337.
52. Ortega,D.R., Yang,W., Subramanian,P., Mann,P., Kjaer,A., Chen,S.Y., Watts,K.J., Pirbadian,S., Collins,D.A., Kooger,R. *et al.* (2020) Repurposing a chemosensory macromolecular machine. *Nat. Commun.*, **11**, 13.
53. Gao,H.C., Yang,Z.M.K., Wu,L.Y., Thompson,D.K. and Zhou,J.Z. (2006) Global transcriptome analysis of the cold shock response of*Shewanella oneidensis* MR-1 and mutational analysis of its classical cold shock proteins. *J. Bacteriol.*, **188**, 4560–4569.
54. Szurmant,H. and Ordal,G.W. (2004) Diversity in chemotaxis mechanisms among the bacteria and archaea. *Microbiol. Mol. Biol. Rev.*, **68**, 301–319.
55. Hess,J.F., Oosawa,K., Kaplan,N. and Simon,M.I. (1988) Phosphorylation of three proteins in the signaling pathway of bacterial chemotaxis. *Cell*, **53**, 79–87.
56. Barak,I. and Youngman,P. (1996) SpoIIE mutants of *Bacillus subtilis* comprise two distinct phenotypic classes consistent with a dual functional role for the SpoIIE protein. *J. Bacteriol.*, **178**, 4984–4989.
57. Adler,E., Donella-Deana,A., Arigoni,F., Pinna,L.A. and Stragler,P. (1997) Structural relationship between a bacterial developmental protein and eukaryotic PP2C protein phosphatases. *Mol. Microbiol.*, **23**, 57–62.
58. Fernandez,P., Saint-Joanis,B., Barilone,N., Jackson,M., Gicquel,B., Cole,S.T. and Alzari,P.M. (2006) The Ser/Thr protein kinase PknB is essential for sustaining mycobacterial growth. *J. Bacteriol.*, **188**, 7778–7784.
59. Alqaseer,K., Turapov,O., Barthe,P., Jagatia,H., De Visch,A., Roumestand,C., Wegrzyn,M., Bartek,I.L., Voskuil,M.I., O'Hare,H.M. *et al.* (2019) Protein kinase B controls *Mycobacterium tuberculosis* growth via phosphorylation of the transcriptional regulator Lsr2 at threonine 112. *Mol. Microbiol.*, **112**, 1847–1862.
60. Dorman,C.J. and Bhriain,N.N. (1992) Thermal regulation of fimA, the *Escherichia coli* gene coding for the type 1 fimbrial subunit protein. *FEMS Microbiol. Lett.*, **99**, 125–130.
61. Colonna,B., Casalino,M., Fradiani,P.A., Zagaglia,C., Naitza,S., Leoni,L., Prosseda,G., Coppo,A., Ghelardini,P. and Nicoletti,M. (1995) H-NS regulation of virulence gene expression in enteroinvasive *Escherichia coli* harboring the virulence plasmid integrated into the host chromosome. *J. Bacteriol.*, **177**, 4703.
62. Dilweg,I.W. and Dame,R.T. (2018) Post-translational modification of nucleoid-associated proteins: an extra layer of functional modulation in bacteria? *Biochem. Soc. Trans.*, **46**, 1381–1392.
63. Hu,L., Kong,W., Yang,D., Han,Q., Guo,L. and Shi,Y. (2019) Threonine phosphorylation fine-tunes the regulatory activity of histone-like nucleoid structuring protein in *Salmonella* transcription. *Front. Microbiol.*, **10**, 1515.
64. Choi,J. and Groisman,E.A. (2020) *Salmonella* expresses foreign genes during infection by degrading their silencer. *Proc. Natl. Acad. Sci. U.S.A.*, **117**, 8074–8082.
65. Castang,S. and Dove,S.L. (2010) High-order oligomerization is required for the function of the H-NS family member MvaT in *Pseudomonas aeruginosa*. *Mol. Microbiol.*, **78**, 916–931.
66. Ueguchi,C., Seto,C., Suzuki,T. and Mizuno,T. (1997) Clarification of the dimerization domain and its functional significance for the *Escherichia coli* nucleoid protein H-NS. *J. Mol. Biol.*, **274**, 145–151.
67. Yamanaka,Y., Winardhi,R.S., Yamauchi,E., Nishiyama,S.I., Sowa,Y., Yan,J., Kawagishi,I., Ishihama,A. and Yamamoto,K. (2018) Dimerization site 2 of the bacterial DNA-binding protein H-NS is required for gene silencing and stiffened nucleoprotein filament formation. *J. Biol. Chem.*, **293**, 9496–9505.
68. Paytubi,S., Madrid,C., Forns,N., Nieto,J.M., Balsalobre,C., Uhlin,B.E. and Juarez,A. (2004) YdgT, the Hha paralogue in *Escherichia coli*, forms heteromeric complexes with H-NS and StpA. *Mol. Microbiol.*, **54**, 251–263.
69. Beltramini,A.M., Mukhopadhyay,C.D. and Pancholi,V. (2009) Modulation of cell wall structure and antimicrobial susceptibility by a *Staphylococcus aureus* eukaryote-like serine/threonine kinase and phosphatase. *Infect. Immun.*, **77**, 1406–1416.
70. Kang,C.M., Abbott,D.W., Park,S.T., Dascher,C.C., Cantley,L.C. and Husson,R.N. (2005) The *Mycobacterium tuberculosis* serine/threonine kinases PknA and PknB: substrate identification and regulation of cell shape. *Genes Dev.*, **19**, 1692–1704.